Experimental measurements and modelling of vapor-liquid equilibria for four mixtures of 2,3,3,3-tetrafluoropropene (R1234yf) with 1,1,1,2-tetrafluoroethane (R134a) or 1,1-difluoroethane (R152a) or trans-1-chloro-3,3,3-Trifluoropropene (R1233zd(E)) or 2-Chloro-3,3,3-trifluoropropene (R1233xf)

Jamal El Abbadi, Christophe Coquelet, Alain Valtz, Céline Houriez

Experimental measurements and modelling of vapor-liquid equilibria for four mixtures of 2,3,3,3-tetrafluoropropene (R1234yf) with 1,1,1,2-tetrafluoroethane (R134a) or 1,1-difluoroethane (R152a) or trans-1-chloro-3,3,3-Trifluoropropene (R1233zd(E)) or 2-Chloro-3,3,3-trifluoropropene (R1233xf)

Jamal El Abbadi[a], Christophe Coquelet[a,b], Alain Valtz[a], Céline Houriez[a]

[a]*MINES ParisTech, PSL University, CTP – Centre of Thermodynamics of Processes, 35 rue Saint Honoré, 77305 Fontainebleau Cedex, France*
[b] *Université de Toulouse, IMT Mines Albi, UMR CNRS 5302, Centre RAPSODEE, Campus Jarlard, 81013 Albi CT Cedex 9, France*

Abstract

Isothermal vapour-liquid equilibrium (VLE) for four binary systems involving R1234yf (R1234yf + R134a, R1234yf + R152a, R1234yf + R1233zd(E) and R1234yf + R1233xf) were measured at temperatures from 278.15 to 348.15 K. The experiments were conducted by means of a "static-analytic" apparatus with phase analysis via gas chromatography, with resulting uncertainties of 0.6 K for temperature, 8 kPa for pressure and a maximum of 0.007 for vapour and liquid mole fractions. The main advantage of the equipment is that vapour and liquid samples are taken from vapour and liquid phase by two capillary samplers (ROLSI®). The Peng Robinson Equation of state is considered to represent the experimental data. If possible, comparison between the new experimental data and prediction with REFPROP 10.0 software are realized.

Keywords: Working fluids, Hydrofluoroolefins, Hydrofluorocarbons, vapor-liquid equilibrium, modeling

Symbols and abbreviations

a	Cohesive energy parameter ($J.m^3.mol^{-2}$)
AAD	Average Absolute deviation
b	Covolume parameter ($m^3.mol^{-1}$)
COP	Coefficient of performance
F_{obj}	Objective function
k_{ij}	Binary interaction parameter (BIP)
m_n	α-function's parameter
MC	Mathias-Copeman
n	Mole number
N	Number of component or experimental data
P	Pressure (MPa) / 1MPa = 10^6 Pa
p	Purity
PR EoS	Peng-Robinson Equation of State
R	Gas constant ($J.mol^{-1}.K^{-1}$)
T	Temperature (K)
u	Uncertainty
v	Molar volume ($m^3.mol^{-1}$)
X	Properties (pressure or mole fraction)
x	Liquid mole fraction
y	Vapor mole fraction
GWP	Global warming potential
HFCs	Hydrofluorocarbons
HFOs	Hydrofluoro-olefins
ODP	Ozone depletion potential

Greek letters

ω	Acentric factor
α	α-function
σ	Standard deviation
Ω_a, Ω_b	Substance depending factors

Subscripts

C	Critical property
cal	Calculated property

exp	Experimental property
i,j	Molecular species
data	Related to the data

Superscripts

V	Vapor phase
L	Liquid phase

1. Introduction

In the previous years, hydrofluorocarbons (HFCs) were used as alternative refrigerants in many industrial applications, due mainly to their thermophysical properties and their zero ozone depletion potential (ODP). Nevertheless, many HFCs have a global warming potential (GWP) greater than 150 and their use will probably be restricted in the upcoming years according to the European Union's F-Gas regulations (Brown et al (2010), Directive 2006/40/EC, European Union Regulation (EC) No 842/2006).

More recently, hydrofluoroolefins (HFOs) have been introduced as replacement fluids to the HFCs thanks to their low GWP and their similar thermophysical properties. In particular, the 1,1,1,2-tetrafluoroethane (HFC-134a or R134a), which is widely used in automotive air conditioning, is gradually replaced by the 2,3,3,3-tetrafluoropropene (HFO-1234yf or R1234yf) which has a low GWP of 4 (Minor and Spatz, 2008) and similar thermophysical properties to those of R134a. Considering the environmental point of view, HFOs are unsaturated HFCs that have high reactivity and therefore shorter lifetimes in the atmosphere. Considering the mechanical engineering point of view, the latent heat of R1234yf is very low, which leads to larger mass flow rates, larger pressure drops in heat exchangers and connection pipes, and eventually, to lower coefficients of performance (COP). One approach to resolve this issue is to use a mixture of R1234yf with other refrigerants like HFCs, such as R134a or 1,1-difluoroethane (R152a).

For instance, R152a which has a GWP of 140 and a short atmospheric lifetime of 1.5 years (McCulloch, 1999), has been used for many years as a component in blends, and its latent heat is much larger than the R1234yf one. Also, mixing more than 36 wt% R134a with R1234yf has an additional advantage to cancel the mild flammability of R1234yf (Yamada et al., 2010).

Furthermore, the mixtures of R1234yf with either R134a or R152a are characterized by the presence of a maximum-pressure azeotrope, which presents advantages for many industrial applications (refrigeration, heat pumps...), as to avoid an important temperature glide. These mixtures can be considered as candidate as working fluid for refrigeration and can be considered as very advantageous in the case of retrofit application in the case where lifespan of installation is very important with respect to F-gas regulations (Lasserre et al. 2014). The phase equilibrium properties of the mixtures of these refrigerants are crucial for an investigation of their performance in refrigeration or the heat pump cycles.

For other applications like high temperature heat pump or Organic Rankine Cycle (ORC), working fluid with high critical point temperature value is highly recommended. Unfortunately, it signifies the utilization of HFCs with high GWP values. Also, considering the technical point of view, utilization of high latent heat and high-density fluid in order to decrease the size of heat exchangers are recommended (Liu et al., 2012). R1233zd(E) (trans-1-chloro-3,3,3-trifluoroprop-1-ene) is one of the most promising compounds (and can be used to replace R245fa). In order to better optimize the performance of heat pump or ORC, it can be judicious to use a blend. Another advantage of blends concerns the temperature glide which is very interesting when we use hot or cold sources with some variation of temperature. The blend composed of R1234yf + R1233zd(E) can be investigated. In this case, vapour liquid equilibrium (VLE) data are essential for the parametrization of equation of state for the prediction of phase diagrams.

Finally, HFOs such as R1234yf have to be produced. According to (Teinz et al., 2015), R1233xf can be used as raw materials to synthesize R1234yf. The design of the separation column, important for the purification process, requires vapour-liquid equilibrium data. R1233xf can also be used as refrigerant and can be associated with R1234yf in a blend.

To the best of our knowledge, very few publications are available in the literature about VLE data of the systems R1234yf + R134a (Kiamika et al., 2013) and R1234yf + R152a [(Hu et al., 2014) and (Yang et al., 2018)]. Also, there is no data concerning the binary system R1234yf + R1233zd(E) and one set of data published by Yang et al. (2016) on the binary system R1234yf + R1233xf.

Regarding the nature of chemicals, all of these systems can be classified as type one according to Scott and van Konynenburg classification (Scott and van Konynerburg, 1980). For such system, Coquelet and Richon (2009) have recommended to use an experimental technique based on static-analytic method (Coquelet et al., 2019).

In this study, the VLE of four systems, R1234yf + (R134a or R152a or R1233zd(E) or R1233xf) were measured using a “static-analytic” apparatus at temperatures T = 278.15 to 343.15 K. To correlate the VLE data and considering the type of phase diagram, the Peng-Robinson (PR-EoS) associated with the Mathias-Copeman α-function and classical mixing rules was considered. Comparison was also done, if possible, with REFPROP 10.0 predictions. Indeed, R1233xf is not available in the software and for the binary system R1234yf + R1233zd(E), no mixing rule parameters are available (alternative mixing rule parameters are considered, i.e. the ones for R1234yf + R1234ze(E) binary system).

2. Experimental

2.1.Materials

Five refrigerants were used for the vapour-liquid equilibrium (VLE) and density measurements. They are listed in Table 1, along with the details about their *ASHRAE* number, chemical formula, *CAS* number, the name of the supplier and the product purity given by the supplier. No further purification of the chemical products was needed, only degassing was realised when loading the chemicals into the equilibrium cell.

Table 1. Refrigerants used for the experimental measurements

Compounds	*ASHRAE[a] Number*	*Formula*	*CAS[b] Number*	*Supplier*	*Purity[c] (vol%)*
1,1,1,2-Tetrafluoroethane	R134a	$C_2H_2F_4$	811-97-2	Climalife	>99%
1,1-Difluoroethane	R152a	$C_2H_4F_2$	75-37-6	Dehon	>99%
2,3,3,3-Tetrafluoropropene	R1234yf	$C_3H_2F_4$	754-12-1	Honeywell	>99.5%
Trans-1-chloro,3,3,3 trifluoropropene	R1233zd(E)	$C_3H_2F_3Cl$	102687-65-0	Synquest	>97%
2-chloro-3,3,3-trifluoropropene	R1233xf	$C_3H_2F_3Cl$	2730-62-3	Synquest	>97%

[a] *ASHRAE: American Society of Heating, Refrigerating and Air-Conditioning Engineers*
[b] *CAS: Chemical Abstracts Service*
[c] from supplier

2.2.Experimental apparatus

The equipment used for the VLE measurements is based on a "static-analytic" method with liquid and vapour phase sampling using capillary samplers ROLSI® (Armines's patent). The equipment can be categorized under "Analytical technique with sampling, isothermal AnT" according to Dohrn classification [(Dohrn et al., 2010) and (Fonseca et al., 2011)].

The equipment is very similar to the one used for the measurement of VLE data concerning the binary systems CO_2 + R1234yf (Juntarachat et al., 2014), CO_2 + R1234ze(E) (Wang et al., 2019) and R1234yf + R245cb (Valtz et al, 2019). The main part of the apparatus is the equilibrium cell, where the two-phase equilibrium takes place. The flow diagram of the apparatus is displayed in Figure 1.

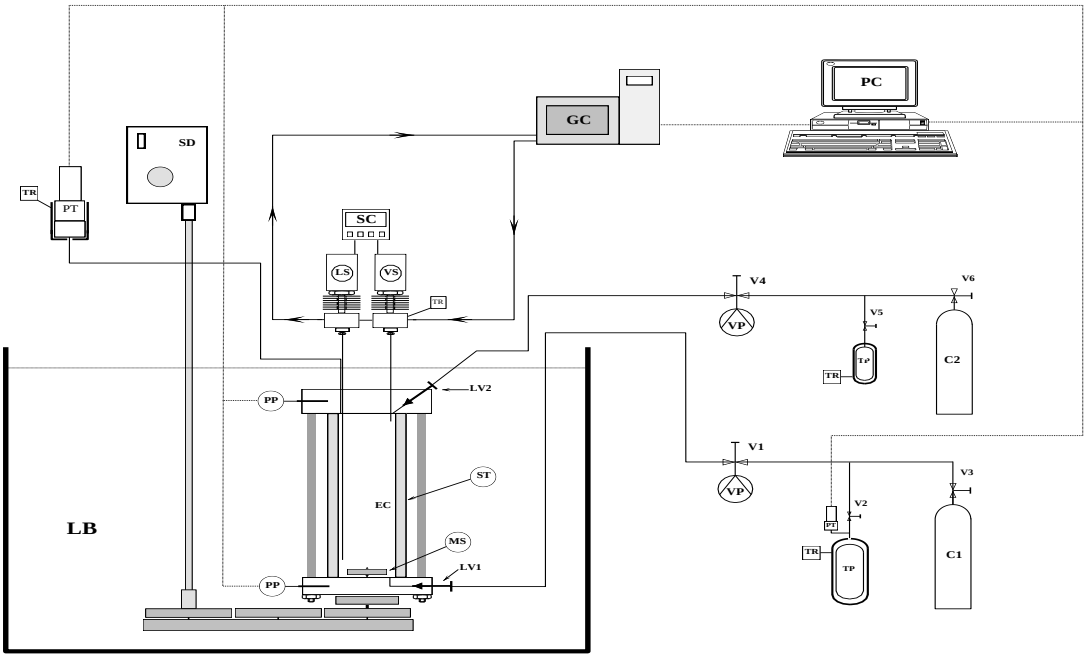

Figure 1. Flow diagram of the "static-analytic" apparatus. EC: equilibrium cell; LV: loading valve; MS: magnetic stirrer; PP: platinum resistance thermometer probe; PT: pressure transducer; RT: temperature regulator; LB: liquid bath; TP: thermal press; C1: more volatile compound; C2: less volatile compound; V: valve; GC: gas chromatograph; LS: liquid sampler; VS: vapor sampler; SC: sample controlling; PC: personal computer; VP: vacuum pump.

The apparatus is equipped with a thermo-regulated liquid bath where the equilibrium cell is immersed. The bath ensures the control of the temperature within 0.01 K.

The temperature measurements inside the equilibrium cell is performed using two platinum resistance thermometer probes (Pt100), one to measure the temperature at the top of the cell, and the other for the temperature at the bottom of the cell. Two other temperature probes are used to control the temperature inside the thermal presses used to load the chemical products into the equilibrium cell.

The Pt100 probes are connected to a data acquisition unit (HP34970A). The Pt100 probes are calibrated against a 25 Ω reference platinum resistance thermometer (Pt25 - Hart Scientific). The Pt25 reference probe was calibrated by the "Laboratoire National d'Essais de Paris" based on the 1990 International Temperature Scale (ITS 90). The temperature accuracy is estimated to be within ± 0.03 K.

The pressure is measured using one of two pressure transducers (DRUCK, 0 – 3 MPa, 0 – 30 MPa) installed on the apparatus. The choice of pressure transducer is dependent upon the maximum pressures generated by the system being characterised. The two pressure transducers are also connected to the data acquisition unit (HP34970A). The pressure transducers were calibrated against a pressure automated calibrator (GE Sensing, model PACE 5000). The pressure accuracy of the transducers is estimated to be within ± 0.0004

MPa. Type B uncertainties were considered for the determination of temperature and pressure uncertainties.

The molar compositions of the phases present within the cell are determined after analysis of liquid and vapour samples by a gas chromatograph (VARIAN, model CP-3800) equipped with a thermal conductivity detector (TCD). The analytical column within the gas chromatograph is a RESTEK, 1% RT-1000 on Carboblack B, 60/80 mesh (length: 2.4m, diameter: 2 mm from Restek, ID Silcosteel).

The TCD is calibrated by introducing manually known amounts of each pure compound (for the system studied) into the injector of the gas chromatograph, using an automatic syringe. The calibration equation was fitted to relate the response of the TCD to the amount of the component introduced. The relative accuracy for each mole number is given in Table 2.

Table 2: Mole number relative accuracy (in %) of TCD for each component.

Binary system	Component 1	Component 2
R1234yf(1) + R134a(2)	0.7	0.7
R1234yf(1) + R152a(2)	0.7	1.0
R1234yf(1) + R1233zd(E)(2)	0.6	1.8
R1234yf(1) + R1233xf(2)	1.2	1.0

The determination of the uncertainty of the mole numbers (Taylor and Kuyatt, 2009) takes into account the repeatability of the measurement, the calibration of the TCD and the purity of the chemicals. The molar fraction is determined from the number of moles of each compound in the analysed sample, given by $x_1 = \frac{n_1}{n_1+n_2}$ for the liquid phase. The uncertainty of mole numbers is given by considering the calibration results (Table 2) and the purity of the chemicals. By definition, we can calculate the uncertainty on mole fraction by considering the relative uncertainties on each mole numbers determined by gas chromatograph after calibration (combined uncertainties). Uncertainty of type B is considered (see Eq. (1)).

$$u^2(x_1) = \left(\frac{\partial x_1}{\partial n_1}\right)^2 u^2(n_1) + \left(\frac{\partial x_1}{\partial n_2}\right)^2 u^2(n_2) = x_1^2(1-x_1)^2\left(\left(\frac{u(n_1)}{n_1\sqrt{3}}\right)^2 + \left(\frac{u(n_2)}{n_2\sqrt{3}}\right)^2\right) \quad (1)$$

Concerning the purity of the chemicals, we consider that it is not correlated to the mole number sensitivity coefficient (equal to one). The uncertainty due to the purity is considered as type B by $u_{pur}(n_i) = \frac{1-p}{\sqrt{3}}$ where p is the purity. Consequently, the global uncertainty is given by Eq. (2).

$$u(x_1) = \sqrt{u_{rep}^2(x_1) + x_1^2(1-x_1)^2\left(\left(\frac{u(n_1)}{n_1\sqrt{3}}\right)^2 + \left(\frac{u(n_2)}{n_2\sqrt{3}}\right)^2 + u_{pur}^2(n_1) + u_{pur}^2(n_2)\right)} \quad (2)$$

$u_{rep}(x_1)$ is due to repeatability, so it is a type A uncertainty given by Eq. (3) (standard deviation).

$$u_{rep}(x_1) = \sqrt{\frac{1}{N_{data}(N_{data}-1)}\sum_{k=1}^{N_{data}}(x_{1\_k} - \bar{x}_1)^2} \quad (3)$$

The uncertainty on relative volatility is given by Eq. (S1) in Supplementary Material.

2.3. Experimental procedure

At ambient temperature, the equilibrium cell and its loading lines are made under vacuum. A first thermal press is loaded with one of the compounds, the second press with the other compound. The liquid bath is set to the temperature desired. When the equilibrium temperature is reached (the equilibrium temperature is reached when the Pt100 probes give the same temperature value within their temperature uncertainty for at least 10 minutes), an amount of about 5 cm^3 of the heavier component (the component with the lower vapour pressure) is introduced into the equilibrium cell. Its vapour pressure is then measured at this temperature.

Then, given amount of the lightest component (the component with the higher vapour pressure) is introduced step by step in order to increase the pressure inside the cell, leading to successive equilibrium mixtures, in order to have enough points to cover the two-phase envelope.

The equilibrium inside the cell is assumed to be reached when the pressure does not change during a period of 10 minutes within ±0.001 MPa under continuous stirring.

For each equilibrium condition, six or more samples of both vapour and liquid phases are taken using the capillary sampler ROLSI® (ARMINES's patent) and analysed in order to verify the repeatability of the measurements, as to have a standard deviation less than 1%.

3. Experimental measurements

The VLE measurements of four binary mixtures have been carried out in this work, considering three isotherms for each mixture. The binary systems studied are R1234yf + R134a, R1234yf + R152a, R1234yf + R1233zd(E) and R1234yf + R1233xf.

3.1.Binary mixture R1234yf + R134a

This system was studied at three isotherms ranging from 278.17 to 333.17 K. The experimental VLE results for this system, along with the number of samples (n), the standard deviation (σx_1 and σy_1) and the measurements uncertainties are provided in Table 3.

Table 3. Vapor Liquid Equilibrium data for the binary system R1234yf (1) + R134a (2) and modelling results.

Experimental data							PR EoS	
P/MPa	***n*** [a]	***x_1***	***σx_1*** [b]	***n***	***y_1***	***σy_1*** [b]	***Pcal/MPa***	***y_{1cal}***
T = 278.17 K								
0.3505	-	0	-	-	0	-	0.3490	0
0.3565	8	0.0541	0.00022	9	0.0672	0.00025	0.3554	0.0672
0.3645	8	0.1450	0.00029	7	0.1698	0.00032	0.3641	0.1698
0.3682	5	0.1878	0.00027	5	0.2154	0.00035	0.3676	0.2154
0.3770	5	0.3488	0.00026	5	0.3735	0.00067	0.3770	0.3735
0.3811	6	0.4736	0.00024	7	0.489	0.00039	0.3812	0.4890
0.3827	7	0.6136	0.0001	6	0.616	0.00032	0.3830	0.6160
0.3827	6	0.6663	0.00019	6	0.6649	0.0003	0.3829	0.6649
0.3822	6	0.7219	0.00016	7	0.7163	0.00033	0.3824	0.7163
0.3814	5	0.7696	0.00011	4	0.7612	0.00018	0.3816	0.7612
0.3813	6	0.7738	0.00007	6	0.7663	0.00058	0.3815	0.7663
0.3807	5	0.8051	0.00004	5	0.7962	0.00023	0.3808	0.7962
0.3781	5	0.8868	0.00009	6	0.8779	0.00044	0.3741	0.9726
0.3744	6	0.9756	0.00007	6	0.9726	0.00008	0.3781	0.8779
0.3735	-	1	-	-	1	-	0.3728	1
T = 303.16 K								
0.7721	-	0	-	-	0	-	0.7695	0
0.7812	6	0.0516	0.00008	4	0.0595	0.00005	0.7789	0.06052
0.7891	8	0.1085	0.00038	4	0.1231	0.00052	0.7878	0.1234
0.7963	7	0.1607	0.00015	8	0.1766	0.00038	0.7960	0.8792
0.8043	3	0.2481	0.00014	4	0.2653	0.00045	0.8038	0.2657
0.8131	7	0.4083	0.00017	4	0.4176	0.00062	0.8135	0.4171
0.8127	3	0.4087	0.0003	3	0.4169	0.00031	0.8135	0.4175
0.8145	4	0.5508	0.00037	11	0.5487	0.00027	0.8153	0.5486
0.8150	4	0.5531	0.00014	4	0.5519	0.0007	0.8152	0.5508
0.8095	4	0.7124	0.00095	4	0.7018	0.00129	0.8102	0.7008
0.8098	3	0.7194	0.00093	2	0.7081	0.00039	0.8098	0.7076
0.8034	5	0.8113	0.00024	11	0.799	0.00062	0.8034	0.7983
0.7963	4	0.8897	0.00023	4	0.8797	0.00018	0.7947	0.1783
0.7925	4	0.9207	0.00006	4	0.9123	0.00013	0.7926	0.9122
0.7840	-	1	-	-	1	-	0.7826	1

				T = 333.17 K				
1.6887	-	0	-	-	0	-	1.6874	
1.7058	4	0.0566	0.00018	5	0.0610	0.00018	1.7023	0.0615
1.7234	5	0.1714	0.00043	5	0.1767	0.00034	1.7244	0.1797
1.7358	4	0.2811	0.00009	5	0.2854	0.00047	1.7368	0.2871
1.7366	4	0.2908	0.00028	4	0.2956	0.00023	1.7375	0.2964
1.7379	3	0.2987	0.00006	3	0.3032	0.00014	1.7381	0.3040
1.7368	4	0.3355	0.00018	4	0.3387	0.00019	1.7401	0.3391
1.7398	4	0.4524	0.00017	4	0.4501	0.0002	1.7410	0.4499
1.7395	4	0.4585	0.00025	4	0.4559	0.00043	1.7408	0.4557
1.7387	3	0.4603	0.00001	2	0.4583	0.00028	1.7407	0.4574
1.7395	4	0.5076	0.00009	4	0.5018	0.00028	1.7386	0.5021
1.7305	7	0.6199	0.00024	5	0.6085	0.00023	1.7286	0.6094
1.7270	3	0.6334	0.00012	4	0.6232	0.00024	1.7269	0.6224
1.7183	4	0.6971	0.00002	4	0.6850	0.00024	1.7177	0.6845
1.7096	4	0.7614	0.00007	4	0.7486	0.00019	1.7063	0.7483
1.6979	5	0.8188	0.00008	4	0.8073	0.00014	1.6942	0.8064
1.6816	4	0.8778	0.00005	6	0.8690	0.00139	1.6800	0.8677
1.6677	4	0.932	0.00009	4	0.9255	0.00012	1.6653	0.9254
1.6447	-	1	-	-	1	-	1.6447	

Expanded uncertainties (k=2) U(T) = 0.06 K; U(P) = 0.0008 MPa; $U_{max}(z_1)$ = 0.008. [a] n: Number of samples [b] σ: Standard deviation

3.2.Binary mixture R1234yf + R152a

This second system was also studied at three isotherms ranging from 278.18 to 333.29 K. The experimental results for this system, along with the number of samples (n), the standard deviation (σx_1 and σy_1) and the measurements uncertainties are reported in Table 4.

Table 4. Vapor Liquid Equilibrium data for the binary system R1234yf (1) + R152a (2) and modelling results.

Experimental data							*PR EoS*	
P/MPa	***n*** [a]	***x_1***	***σx_1*** [b]	***n***	***y_1***	***σy_1*** [b]	***Pcal/MPa***	***y_{1cal}***
T = 278.18 K								
0.3152	-	0	-	-	0	-	0.3150	
0.3210	7	0.0323	0.00034	7	0.0479	0.00033	0.3210	0.0485
0.3344	7	0.1172	0.00032	10	0.1580	0.00030	0.3344	0.1601
0.3400	7	0.1590	0.00016	6	0.2066	0.00019	0.3400	0.2088
0.3470	7	0.2205	0.00018	8	0.2728	0.00027	0.3472	0.2750
0.3522	6	0.2748	0.00051	9	0.3273	0.00033	0.3527	0.3294
0.3641	4	0.4247	0.00055	5	0.4667	0.00072	0.3643	0.4678
0.3690	8	0.5284	0.00030	6	0.5577	0.00014	0.3698	0.5586
0.3744	6	0.6726	0.00011	5	0.6833	0.00075	0.3745	0.6846
0.3764	7	0.7511	0.00012	8	0.7541	0.00006	0.3756	0.7552
0.3767	7	0.8104	0.00014	6	0.8092	0.00005	0.3759	0.8102
0.3767	6	0.8151	0.00010	6	0.8138	0.00006	0.3759	0.8146
0.3763	7	0.8454	0.00010	5	0.8424	0.00011	0.3758	0.8434
0.3758	9	0.9052	0.00008	9	0.9011	0.00011	0.3751	0.9019
0.3746	5	0.9388	0.00004	5	0.9353	0.00003	0.3745	0.9360
0.3729	-	1	-	-	1	-	0.3729	
T = 303.16 K								
0.6899	-	0	-	-	0	-	0.6906	
0.7079	5	0.0566	0.00012	7	0.0754	0.00014	0.7088	0.0761
0.7380	6	0.1759	0.00015	13	0.2131	0.00027	0.7393	0.2145
0.7571	5	0.2796	0.00016	5	0.3190	0.00012	0.7590	0.3196
0.7766	10	0.4215	0.00022	6	0.4508	0.00013	0.7779	0.4520
0.7861	8	0.5259	0.00027	5	0.5441	0.00019	0.7869	0.5453
0.7912	5	0.5961	0.00080	5	0.6074	0.00016	0.7908	0.6081
0.7933	5	0.6343	0.00061	5	0.6421	0.00017	0.7923	0.6425
0.7961	5	0.7687	0.00024	9	0.7664	0.00023	0.7937	0.7666
0.7952	8	0.7977	0.00023	6	0.7949	0.00013	0.7932	0.7942
0.7922	5	0.8817	0.00017	7	0.8773	0.00014	0.7904	0.8766
0.7896	6	0.9320	0.00007	7	0.9283	0.00014	0.7876	0.9279
0.7835	-	1	-	-	1	-	0.7826	
T = 333.29 K								
1.5083	-	0	-	-	0	-	1.5081	
1.5396	6	0.0580	0.00006	6	0.0699	0.00031	1.5399	0.071
1.5645	6	0.1092	0.00011	5	0.1278	0.00044	1.5643	0.1294
1.5893	5	0.1759	0.00008	6	0.1987	0.00088	1.5917	0.2010
1.6185	10	0.2611	0.00065	6	0.2842	0.00102	1.6202	0.2869
1.6387	8	0.3332	0.00029	7	0.3546	0.00297	1.6395	0.3566
1.6532	6	0.4003	0.00045	8	0.4189	0.00078	1.6537	0.4198
1.6668	8	0.4904	0.00022	9	0.5032	0.00146	1.6677	0.5035
1.6751	7	0.5671	0.00010	6	0.5734	0.00089	1.6753	0.5745

1.6784	6	0.6142	0.00029	9	0.6183	0.00034	1.6780	0.6183
1.6811	7	0.6623	0.00009	5	0.6638	0.00037	1.6794	0.6640
1.6814	5	0.6972	0.00015	6	0.6967	0.00037	1.6795	0.6965
1.6807	9	0.7346	0.00045	6	0.7333	0.00030	1.6787	0.7322
1.6741	10	0.8258	0.00011	6	0.8223	0.00027	1.6733	0.8210
1.6655	7	0.8966	0.00008	8	0.8934	0.00045	1.6657	0.8921
1.6598	12	0.9487	0.00006	7	0.9460	0.00018	1.6581	0.9458
1.6590	17	0.9488	0.00005	5	0.9466	0.00019	1.6581	0.9459
1.6419	-	1	-	-	1	-	1.6492	

Expanded uncertainties (k=2) U(T) = 0.06 K; U(P) = 0.0008 MPa; $U_{max}(z_1)$ = 0.008. [a] n: Number of samples [b] σ: Standard deviation

3.3.Binary mixture R1234yf + R1233zd(E)

This second system was also studied at two temperatures, 303.22 and 333.27 K. The experimental results for this system, along with the number of samples (n), the standard deviation (σx_1 and σy_1) and the measurements uncertainties are reported in Table 5.

Table 5. Vapor Liquid Equilibrium data for the binary system R1234yf (1) + R1233zd(E) (2) and modelling results.

		Experimental data					*PR EoS*	
P/MPa	***n*** [a]	***x_1***	***σx_1*** [b]	***n***	***y_1***	***σy_1*** [b]	***Pcal/MPa***	***y_{1cal}***
				T = 303.22 K				
0.2031	9	0.0567	0.0002	12	0.2477	0.0005	0.1987	0.2505
0.3060	6	0.1895	0.0002	6	0.5379	0.0008	0.2932	0.5445
0.3936	7	0.339	0.004	7	0.696	0.003	0.3899	0.7042
0.4504	10	0.428	0.003	12	0.764	0.001	0.4440	0.7661
0.5032	10	0.5175	0.0005	5	0.813	0.001	0.4966	0.8155
0.6185	6	0.724	0.001	6	0.904	0.001	0.6156	0.9036
0.7198	9	0.895	0.001	9	0.9655	0.0005	0.7173	0.9642
				T = 333.27 K				
0.6159	6	0.1529	0.0004	18	0.403	0.003	0.6249	0.4264
0.8058	6	0.3066	0.0007	10	0.600	0.002	0.8295	0.6146
1.0269	7	0.491	0.001	6	0.750	0.007	1.0498	0.7473
1.1924	7	0.6331	0.0009	8	0.827	0.004	1.2109	0.8233
1.4033	6	0.8121	0.0007	6	0.912	0.003	1.4159	0.9084
1.5059	5	0.8960	0.0008	12	0.942	0.002	1.5166	0.9482

Expanded uncertainties (k=2) U(T) = 0.06 K; U(P) = 0.0008 MPa; $U_{max}(z_1)$ = 0.007. [a] n: Number of samples [b] σ: Standard deviation

3.4.Binary mixture R1234yf + R1233xf

This second system was also studied at three isotherms ranging from 298.31 to 348.25 K. The experimental results for this system, along with the number of samples (n), the standard deviation (σx_1 and σy_1) and the measurements uncertainties are reported in Table 6.

Table 6. Vapor Liquid Equilibrium data for the binary system R1234yf (1) + R1233xf (2) and modelling results.

		Experimental data					PR EoS	
P/MPa	***n*** [a]	***x_1***	***σx_1*** [b]	***n***	***y_1***	***σy_1*** [b]	***Pcal/MPa***	***y_{1cal}***
				T = 298.31 K				
0.3462	6	0.3505	0.0008	10	0.676	0.0005	0.3466	0.6755
0.4490	7	0.551	0.002	6	0.817	0.0008	0.4491	0.8149
0.5389	6	0.7261	0.0008	6	0.8979	0.003	0.5384	0.8988
0.6217	9	0.8824	0.0003	14	0.959	0.001	0.6202	0.9592
0.248	6	0.1709	0.0009	13	0.4518	0.001	0.2521	0.4580
				T = 333.27 K				
0.5004	6	0.1616	0.0008	6	0.386	0.001	0.5008	0.3971
0.7075	6	0.383	0.002	6	0.65	0.002	0.7113	0.6583
1.0664	7	0.767	0.0003	6	0.894	0.001	1.0705	0.8944
1.196	7	0.8975	0.0008	18	0.9541	0.0002	1.1993	0.9545
0.8935	4	0.5863	0.0002	5	0.7986	0.0003	0.9001	0.7999
				T = 348.25 K				
0.9246	6	0.1715	0.0005	8	0.3554	0.0006	0.9179	0.3609
1.1507	18	0.3222	0.0005	8	0.5428	0.0003	1.1484	0.5480
1.3436	5	0.4501	0.0004	6	0.6577	0.002	1.3447	0.6626
1.7659	10	0.7186	0.0006	10	0.8412	0.0007	1.7719	0.8413
2.1343	11	0.9275	0.0004	8	0.9587	0.0004	2.1412	0.9587

Expanded uncertainties (k=2) U(T) = 0.06 K; U(P) = 0.0008 MPa; Umax(z1) = 0.005 [a] n: Number of samples [b] σ: Standard deviation

4. Modelling and discussions

In order to correlate the data, we have considered the most popular cubic equation of state present in all process simulators, the Peng-Robinson equation of state (PR EoS) (Peng and Robinson, 1976). This model is also considered to correlate and check the quality of the experimental. This model doesn't require numerous parameters and is used to generate phase diagrams. The PR EoS is a two-parameter cubic EoS and is defined by Eq. (4).

$$P = \frac{RT}{v-b} - \frac{a(T)}{v^2+2bv+b^2} \quad (4)$$

P is the pressure, T the temperature, v the volume, and R the universal constant for ideal gases. b is the volumetric parameter and a(T) the cohesive energy parameter. The cohesive energy parameter a(T) depends on the temperature and is defined by Eq. (5).

$$a(T) = a_c \alpha(T) \quad (5)$$

The parameters a_c, and b are defined by $a_c = \Omega_a \frac{R^2 {T_c}^2}{P_c}$ and $b = \Omega_b \frac{RT_c}{P_c}$.
In order to have the best prediction of the pure component vapour pressure and considering the fact that all of our experimental data were obtained for temperature lower than the critical temperature of the lightest component, the Mathias-Copeman (Mathias Copeman, 1983) α-function was selected. The α-function is defined by Eq. (6).

$$\alpha(T) = \left[1 + m_1\left(1 - \sqrt{\frac{T}{T_c}}\right) + m_2\left(1 - \sqrt{\frac{T}{T_c}}\right)^2 + m_3\left(1 - \sqrt{\frac{T}{T_c}}\right)^3\right]^2; \quad if\ T < T_c \quad (6)$$

T and T_c are respectively the temperature and the critical temperature. m_1, m_2 and m_3 are three adjustable parameters fitted on the experimental data
For the mixtures, the classical van der Waals (vdW) mixing and combining rules (Kwak and Mansoori, 1986) were used for the calculations. They are defined by Eqs (7-8).

$$a = \sum_{i=1}^{N} \sum_{j=1}^{N} z_i z_j a_{ij} \quad (7)$$

$$b = \sum_{i=1}^{N} z_i b_i \quad (8)$$

With $a_{ij} = \left(1 - k_{ij}\right)\sqrt{a_i a_j}$, $i = 1,2 \ldots . N$, $j = 1,2 \ldots . N$.

z_i is the mole fraction of the component i, a_i is the energy parameter, b_i is the covolume parameter of the component i, and k_{ij} is the binary interaction parameter (BIP). N is the number of components of the system. The vdW mixing rules were chosen for their simplicity, ease of computing and also to be able to use a predictive binary interaction parameter k_{ij}. For the VLE modelling, the model parameters have been adjusted in order to have an accurate representation, especially with the presence of an azeotrope. The binary interaction parameter

(BIP) was fitted on experimental VLE data to take into account the molecular interactions occurring, and the *α-function* parameters m_1, m_2 and m_3 were fitted on the pure compound data, in order to accurately represent the vapour pressures and the critical point.

For the R1234yf + R152a and R1234yf + R134a binary systems, the BIP k_{ij} is fitted on the VLE data of bubble pressure according to the Eq. (9). As there is no important difference between vapour and liquid phase mole fractions, we have preferred to not include mole fraction of vapour phase in the objective function used:

$$F_{obj} = \frac{100}{N_{data}} \left[\sum_1^N \left(\frac{P_{exp} - P_{cal}}{P_{exp}} \right)^2 \right] \quad (9)$$

For the R1234yf + R1233zd(E) and R1234yf + R1133xf binary systems, the BIP k_{ij} is fitted on the VLE data of bubble pressure and mole fraction of vapour according to the Eq. (10).

$$F_{obj} = \frac{100}{N_{data}} \left[\sum_1^{N_{data}} \left(\frac{P_{exp} - P_{cal}}{P_{exp}} \right)^2 + \sum_1^{N_{data}} \left(\frac{y_{1,exp} - y_{1,cal}}{y_{1,exp}} \right)^2 \right] \quad (10)$$

For the Eqs (9-10), N_{data} is the number of data points, P_{exp} the experimental bubble pressure, P_{cal} the calculated bubble pressure, y_{exp} the experimental vapour molar fraction and y_{cal} the calculated vapour molar fraction.

The critical temperature and pressure, and the acentric factor (ω) of these refrigerants are reported in Table 7**.** We have used the pure component vapour pressure predicted by the NIST (REFPROP 10.0, Lemmon et al. (2018)). The relative uncertainties given by the NIST are 0.02 % for R134a, 0.1 % for R152a, 0.1 % for R1234yf and 0.131% for R1233zd(E). For R1233xf, we have considered the experimental data mentioned by Zhang et al., 2013. They claimed a relative uncertainty of 0.5 %. The values of the Mathias-Copeman alpha function parameters for the five single compounds used in this study are provided in Table 8 with the corresponding AAD (Average Absolute Deviation) and Bias. The Mathias Copeman Alpha function is applicable in the whole range or pressure and temperature from 273.15K to the critical temperature. Of course, for temperature higher than the critical temperature higher than the critical temperature, only the first parameter m_1 have to be considered with the adapted expression for $T>T_C$: $\alpha(T) = \left[1 + m_1 \left(1 - \sqrt{\frac{T}{T_c}}\right)\right]^2$). We have used the pure compound

vapour pressures predicted by REFPROP 10.0. For the R1233xf, we have considered the experimental data measured by Zhang et al. The results are also presented in Supplementary Materials (ln(P) as a function of 1/T and the deviations, Figures S1 to S10).

Table 7. Critical properties and acentric factor values from REFPROP (Lemmon et al., 2018) of the refrigerants studied.

Component	T_c/K	P_c/MPa	ω
1,1,1,2-Tetrafluoroethane, R134a	374.21	4.05928 [	0.3268
1,1-Difluoroethane, R152a	386.41	4.51675	0.2752
2,3,3,3-Tetrafluoropropene, R1234yf	367.85	3.3822	0.2760
trans-1-chloro-3,3,3-Trifluoropropene, R1233zd(E)	439.60	3.6237]	0.3025
2-chloro-3, 3, 3-trifluoropropene, R1233xf	439.98[a]	3.32201 [a]	0.1873 [a]

[a] Zhang et al. (2013)

Table 8. Mathias Copeman alpha function parameters adjusted for each pure component (range of Temperature from 273.15 K to the pure component critical temperature)

Component	m_1	m_2	m_3	AAD /%	Bias /%
R1234yf	0.80519	-0.33942	1.01599	0.16	-0.04
R134a	0.85811	-0.13358	0.49210	0.27	-0.13
R152a	0.81002	-0.45981	1.59189	0.19	-0.18
R1233zd(E)	0.85356	-0.53966	1.80195	0.13	-0.02
R1233xf	0.31079	3.51330	-8.73344	0.44	0.02

4.1.Binary mixture R1234yf + R134a

The results of the modelling for the system R1234yf + R134a are displayed in Figure 2 (T = 278.17 K) and Figures S11 to S13 for the other temperatures, from which we can notice that the model, in overall, reproduces accurately the experimental results. The calculated values by our model are given in Table 3. This system exhibits an azeotropic behaviour, which can be expected due to the close values of the vapour pressures of the two refrigerants R1234yf and R134a. Also, we can observe that the VLE diagram is very narrow, due to the close mole fraction values of the vapour and liquid phases, which makes the modelling quite challenging. In order to check our measurements, the relative volatility was calculated (Figure 3). We can verify that the relative volatility is a decreasing function of the mole fraction of liquid phase and is equal to one at the composition of the azeotrope.

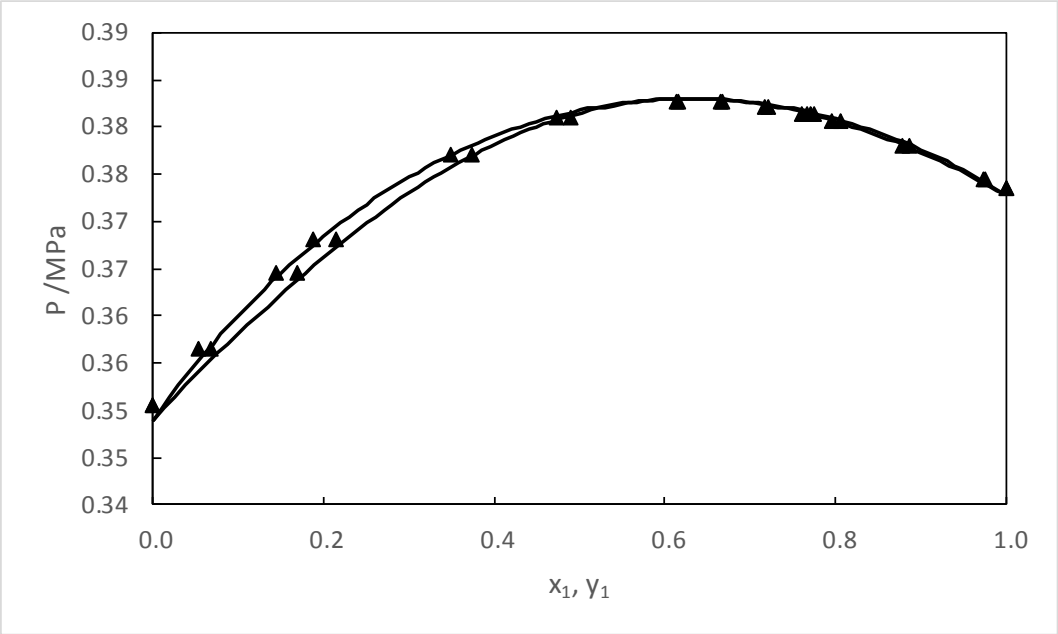

Figure 2. Phase diagrams for the R1234yf + R134a binary system at (▲) 278.17 K. Solid line: modelling results using the Peng Robinson EoS.

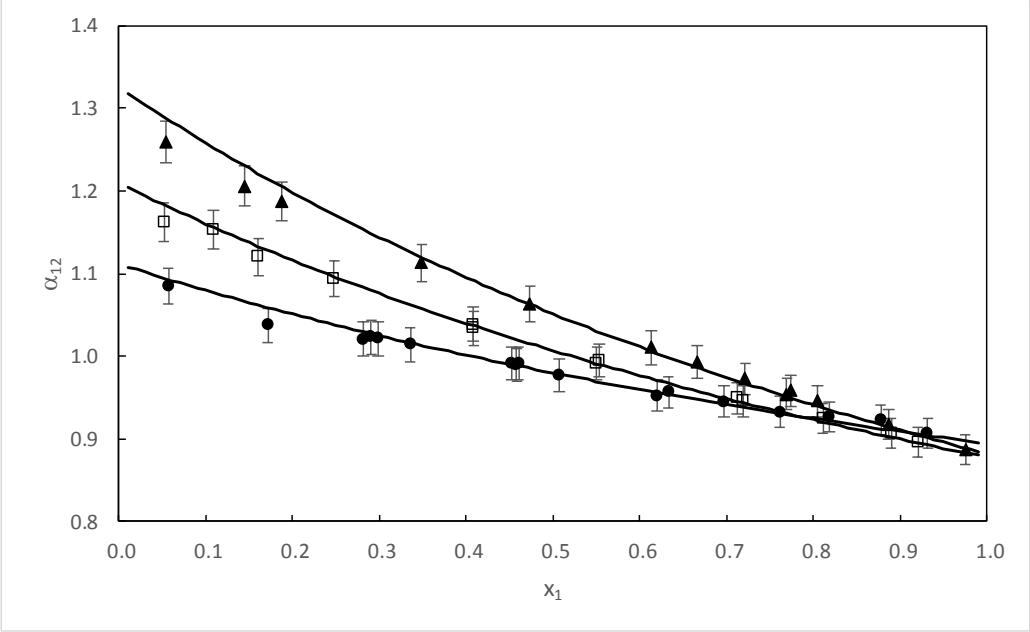

Figure 3. Relative volatility of the (R1234yf + R134a) binary system at (▲) 278.17 K; (□) 303.16 K and (●) 333.17 K; solid line: modelling results using the Peng-Robinson EoS. Error bars (uncertainty on relative volatility): 2 %

In Table 9, we report the results of the AAD and bias calculated for the bubble pressure and the mole fraction of vapour phase, along with the values of the BIP fitted on the experimental data. The AAD and bias are calculated according to Eqs. (11-12).

$$AAD(X)\ \% = \frac{100}{N}\left|\sum_1^N \frac{X_{exp}-X_{cal}}{X_{exp}}\right| \quad (11)$$

$$Bias\ (X)\ \% = \frac{100}{N}\sum_1^N \frac{X_{exp}-X_{cal}}{X_{exp}} \quad (12)$$

In addition to the data measured as part of this work, the VLE data from the literature (Kamiaka et al.) were modelled by using the same thermodynamic model, and the results of the AAD and bias were reported as well in Table 9. We have also compared our results and those from Kamiaka et al. with the prediction given by REFPROP. In REFPROP 10.0, some mixing parameters are proposed for this binary system. We can observe that there is a good agreement between our data and literature data if we compare the values of binary interaction parameters (Figure 4) obtained after adjustment. But we can also see that the trend concerning the variation of the BIP with the temperature is different between our data and those from Kiamiaka et al. Moreover, concerning the data from Kiamiaka et al., we can observed that there are systematic deviation between experimental and calculated mole fraction of vapour phase values. The deviations between the experimental data and predictions from REFPROP are higher than the deviations obtained using the PR EoS.

Table 9. Deviations between the experimental data and modelling results (AAD and bias) for the binary system R1234yf (1) + R134a (2).

			PR EoS				REFPROP			
Reference	***T/K***	k_{12}	***AAD P /%***	***AAD y_1 /%***	***bias P /%***	***bias y_1 /%***	***AAD P /%***	***AAD y_1 /%***	***bias P /%***	***bias y_1 /%***
This work	*278.17*	*0.0178*	*0.11*	*0.49*	*0.06*	*-0.33*	*0.52*	*0.35*	*-0.49*	*0.71*
	303.16	*0.0184*	*0.11*	*0.29*	*0.06*	*-0.19*	*0.49*	*0.40*	*-0.47*	*0.59*
	333.17	*0.0189*	*0.10*	*0.28*	*0.01*	*-0.19*	*0.28*	*0.53*	*-0.18*	*0.40*
Kamiaka et al. 2013	*273.33*	*0.0203*	*0.29*	*0.14*	*0.15*	*-0.07*	*0.28*	*0.29*	*0.04*	*0.18*
	283.16	*0.0201*	*0.25*	*0.67*	*0.14*	*-0.67*	*0.26*	*0.73*	*-0.12*	*0.73*
	293.14	*0.0198*	*0.21*	*0.34*	*0.12*	*-0.34*	*0.26*	*0.73*	*-0.12*	*0.73*
	303.17	*0.0185*	*0.14*	*0.46*	*0.04*	*-0.17*	*0.44*	*0.64*	*-0.41*	*0.63*
	313.18	*0.0181*	*0.17*	*0.46*	*0.04*	*-0.46*	*0.45*	*0.84*	*-0.41*	*0.69*
	323.18	*0.0177*	*0.12*	*0.26*	*0.01*	*-0.26*	*0.43*	*0.67*	*-0.38*	*0.37*
	333.18	*0.0166*	*0.13*	*0.13*	*-0.04*	*-0.13*	*0.47*	*0.63*	*-0.43*	*-0.17*

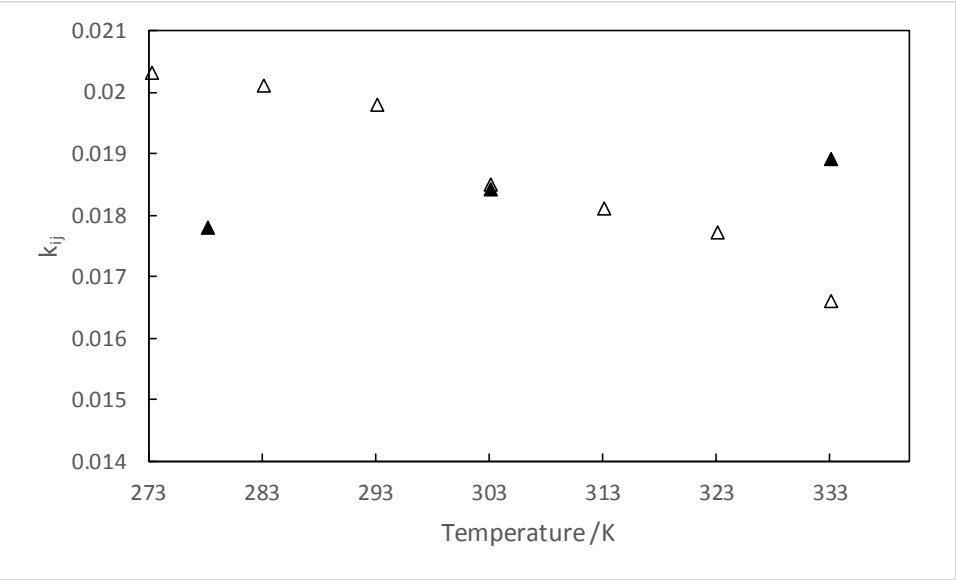

Figure 4: Variation of the binary interaction parameters (binary system R1234yf + R134a) with the temperature. (▲): this work, (Δ): Kamiaka et al.

4.2.Binary mixture R1234yf + R152a

The VLE modelling results for the system R1234yf + R152a are displayed in Figure 5 (T = 278.18 K) and Figures S14 and S16 for the other temperatures, from which we can notice that the calculations are, in overall, in good agreement with the experimental results. The calculated values by our model are given in Table 4. Similarly to the previous system, this binary system has an azeotropic behaviour, which can be expected due to the close values of the vapour pressures of the two refrigerants R1234yf and R152a. Also, we can observe that the VLE diagram is very narrow, due to the close mole fractions of the vapour and liquid phases, which makes the modelling quite challenging. In order to check our measurements, the relative volatility was calculated (Figure 6). We can see that the relative volatility is a decreasing function of the mole fraction of the liquid phase and is equal to one at the composition of the azeotrope.

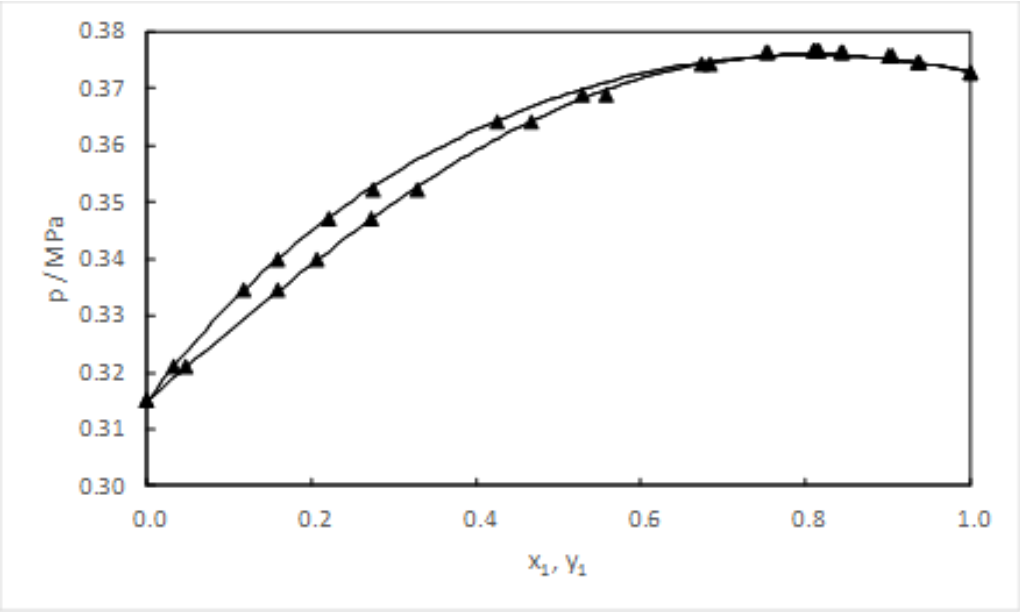

Figure 5. Phase diagrams for the R1234yf + R152a binary system at (▲) 278.18 K Solid line: modelling results using the Peng Robinson EoS.

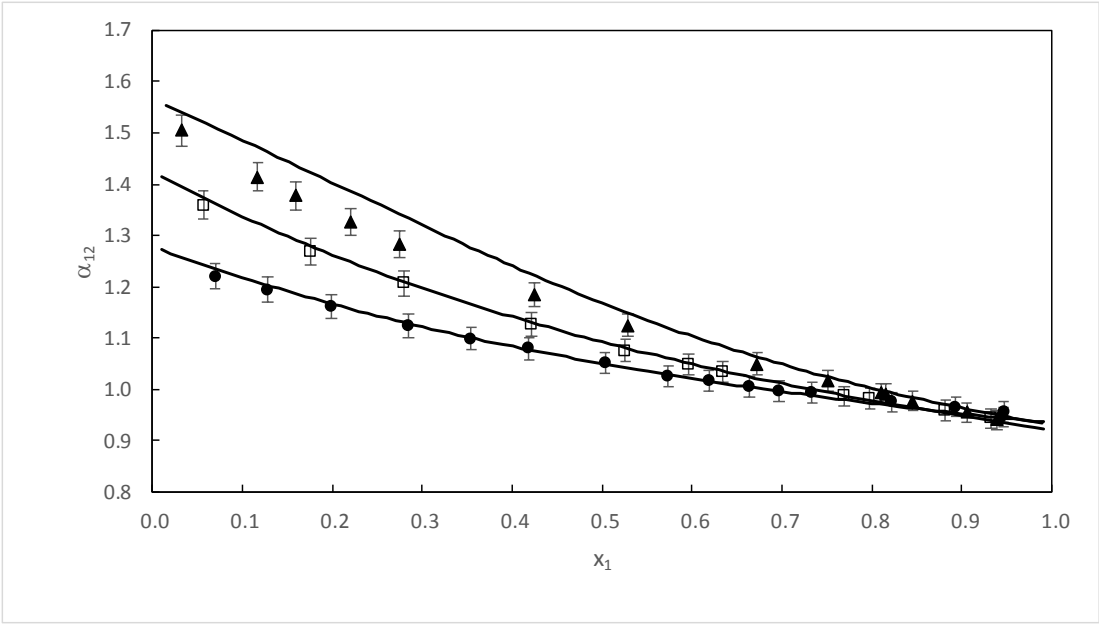

Figure 6. Relative volatility of the (R1234yf + R152a) binary system at (▲) 278.17 K; (□) 303.16 K; (●) 333.17 K; solid line: modelling results using the Peng Robinson EoS. Error bars (uncertainty on relative volatility): 2 %

The results of the AAD and bias calculated for the bubble pressure and the mole fraction of vapour phase, along with the values of the BIP fitted on the experimental data are reported in Table 10. In addition to the data measured in this work, the VLE data from the literature (Hue et al. 2014; Yang et al. 2018) were modelled by using the same thermodynamic model, and the results of the AAD and bias were reported as well in Table 10. We have also compared our results and those from Hu et al. and Yang et al. with the predictions given by REFPROP

where the mixing parameters used are given in the paper of Bell and Lemmon (2016) As we can see, there is a good agreement between our data and literature data if we compare the values of binary interaction parameters (Figure 7). But we can also see that the variation of the BIP with the temperature obtained after data treatment for the three sets of data are similar and not too much temperature dependent (k_{ij} close to 0.02). Also, according to the Table 10, we can observe a systematic deviation concerning the mole fraction of vapour phase for the data measured by Yang et al. The deviations between the experimental data and predictions from REFPROP are higher than the deviations obtained using the PR EoS. The deviations between experimental data from Yang et al. and REFPROP predictions are the highest.

Table 10. AAD and bias for the binary mixture R1234yf (1) + R152a (2).

			PR EoS				***REFPROP***			
Reference	***T/K***	***k_{12}***	***AAD P /%***	***AAD y_1 /%***	***bias P /%***	***bias y_1 /%***	***AAD P /%***	***AAD y_1 /%***	***bias P /%***	***bias y_1 /%***
This work	278.18	0.0171	0.10	0.40	0.03	-0.40	0.31	0.67	-0.22	0.53
	303.16	0.0190	0.17	0.22	0.03	-0.18	0.25	0.29	-0.01	0.14
	333.29	0.0194	0.08	0.39	-0.02	-0.32	0.20	0.45	0.08	0.27
Hu et al. 2014	283.15	0.0193	0.25	0.98	0.08	-0.82	0.22	0.88	0.12	0.64
	293.15	0.0193	0.18	0.87	0.06	-0.65	0.15	0.97	0.04	0.59
	303.15	0.0190	0.18	0.67	0.03	-0.55	0.19	0.73	-0.02	0.50
	313.15	0.0196	0.15	0.80	0.03	-0.61	0.15	0.82	0.06	0.53
	323.15	0.0201	0.13	0.65	0.03	-0.46	0.19	0.69	0.14	0.36
Yang et al. 2018	283.15	0.0195	0.09	0.32	0.03	0.32	0.13	5.44	0.07	-4.48
	293.15	0.0196	0.13	0.14	0.03	0.14	0.13	0.30	0.05	0.17
	303.15	0.0198	0.11	0.14	-0.01	0.10	0.15	0.32	0.03	0.15
	313.15	0.0199	0.11	0.11	0.002	0.11	0.15	0.17	0.05	0.07
	323.15	0.0198	0.11	0.14	-0.02	0.14	0.15	0.17	0.05	0.08

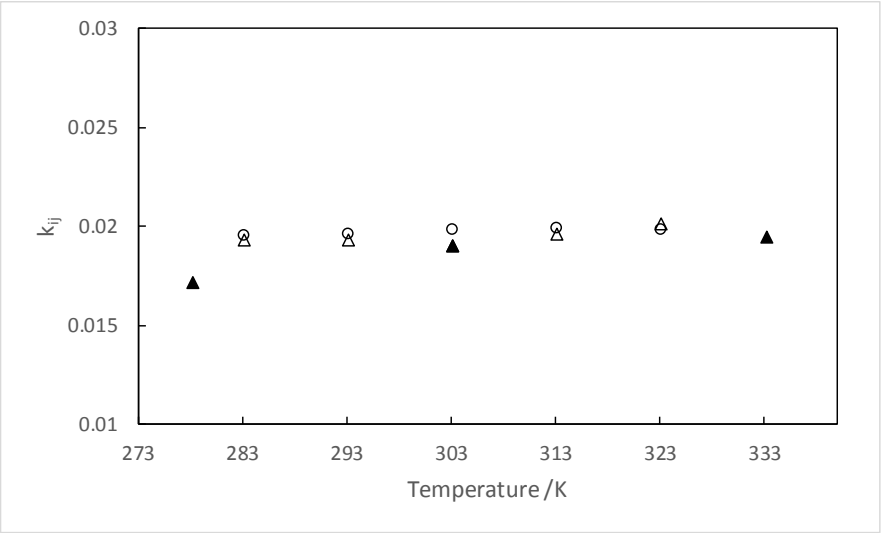

Figure 7: Variation of the binary interaction parameters (binary system R1234yf + R152a with the temperature. (▲): this work; (Δ): Hu et al.; (o): Yang et al..

4.3.Binary mixture R1234yf + R1233zd(E)

The VLE modelling results for the binary system R1234yf + R1233zd(E) are displayed in Figure 8, from which we can notice that the calculations are in good agreement with the experimental results. The calculated values by our model are given in Table 5. There is no azeotrope. In order to check our measurements, the relative volatility was calculated (Figure 9). We can see that the relative volatility is a decreasing function of the liquid molar fraction.

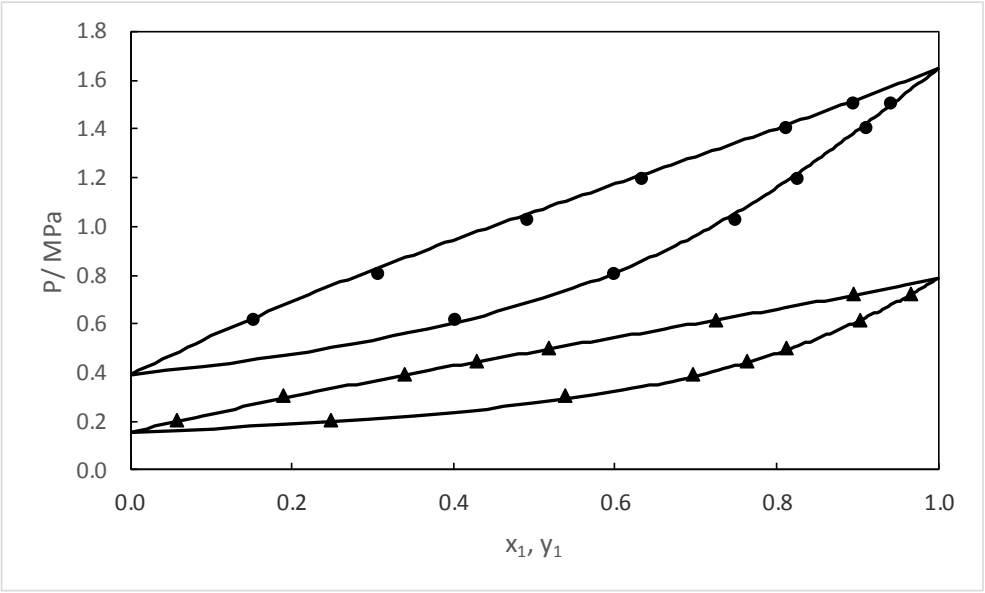

Figure 8. Phase diagrams for the R1234yf + R1233zd(E) binary system at (▲) 303.22 K; (●) 333.27 K; Solid line: modelling results using the Peng Robinson EoS.

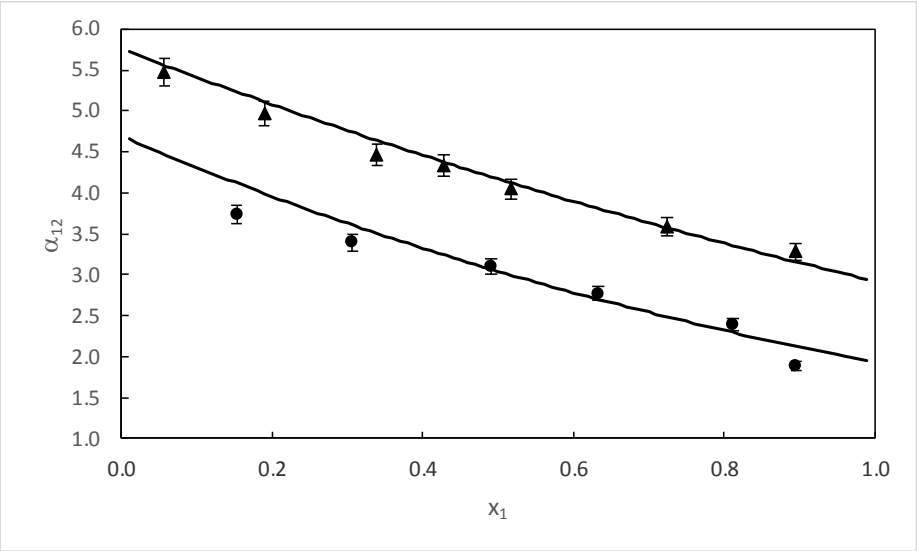

Figure 9. Relative volatility of the R1234yf + R1233zd(E) binary system at (▲) 303.22 K and (●) 333.27 K. Solid line: modelling results using the Peng Robinson EoS. Error bars (uncertainty on relative volatility): 3 %

The results of the AAD and bias calculated for the bubble pressure and the mole fraction of vapour phase, along with the values of the BIP fitted on the experimental data are reported in Table 11. We have also compared our results with the prediction given by REFPROP. Unfortunately, there is no specific mixing parameters for this binary system in REFPROP. In our version of REFPROP, the BIP of the binary system R1234yf + R1234ze(E) are thus considered (similar system). We can observe that the deviations between our model and the experimental data are higher than the deviations between our experimental data and REFPROP's predictions. This can be attributed to the low level of purity of the R1233zd(E) in comparison to the purity of R134a, R1234yf and R152a. One consequence of the presence of impurities is that the deviations are the highest at 333.27 K.

Table 11. AAD and bias for the binary mixture R1234yf (1) + R1233zd(E).

		PR EoS				***REFPROP***			
T/K	***k_{12}***	***AAD P /%***	***AAD y_1 /%***	***bias P /%***	***bias y_1 /%***	***AAD P /%***	***AAD y_1 /%***	***bias P /%***	***bias y_1 /%***
303.22	0.0205	1.5	0.6	1.5	-0.6	0.83	0.92	-0.83	0.55
333.27	0.0358	1.6	1.7	-1.6	-1.3	0.52	0.77	-0.52	0.06

4.4.Binary mixture R1234yf + R1233xf

The VLE modelling results for the system R1234yf + R1233xf are displayed in figure 10, from which we can notice that the calculations are in good agreement with the experimental results. The calculated values by our model are given in Table 6. There is no azeotrope. In order to check our measurements, the relative volatility was calculated (Figure 11). We can see that the relative volatility is a decreasing function of the liquid molar fraction.

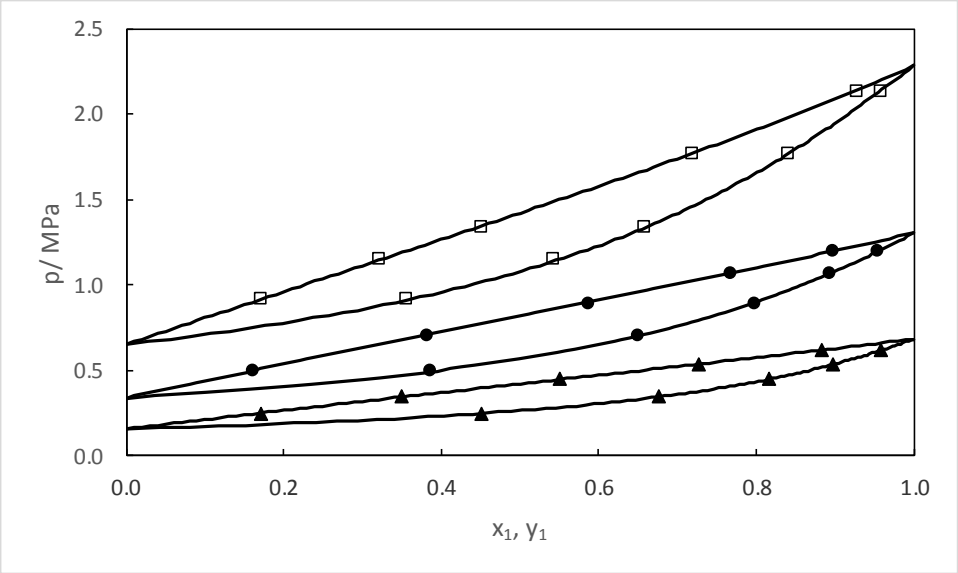

Figure 10. Phase diagrams for the R1234yf + R1233xf binary system at (▲) 298.31 K; (•) 323.27 K (□): 348.25 K. Solid line: modelling results using the Peng Robinson EoS.

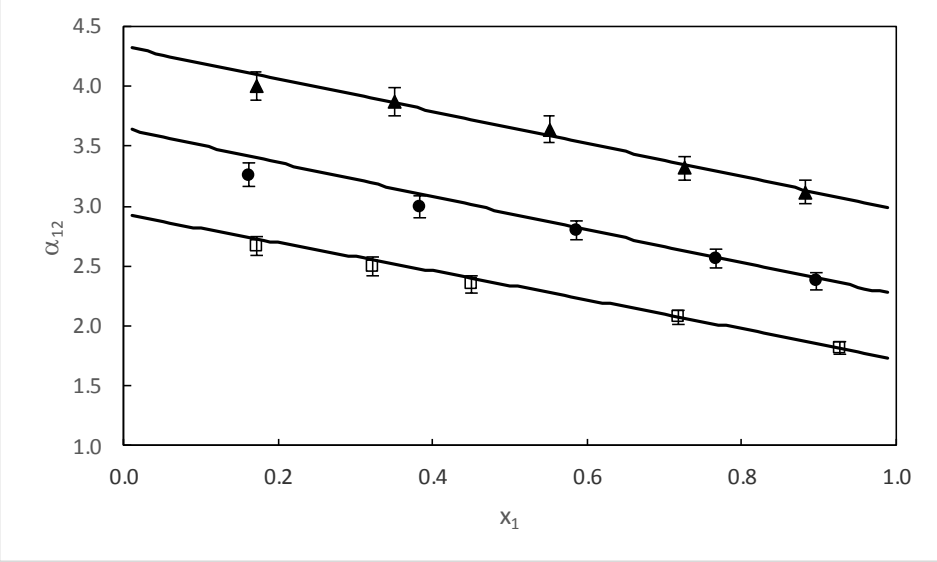

Figure 11. Relative volatility of the R1234yf + R1233xf binary system (▲) 298.31 K; (•) 323.27 K (□): 348.25 K. Solid line: modelling results using the Peng-Robinson Equation of State. Error bar (uncertainty on relative volatility): 3%

The results of the AAD and bias calculated for the bubble pressure and the mole fraction of the vapour phase, along with the values of the BIP fitted on the experimental data are reported in Table 12. We have also compared our results with the results from Yang et al. (2016). The deviations are indicated in the Table12. As the R1233xf is not available in REFPROP 10.0, we do not compare the experimental data with REFPROP predictions. The variations of the BIP with the temperature are plotted on Figure 12. We can see that the orders of magnitude of the BIP are similar, reflecting a good agreement between the two sets of data.

Table 12. AAD and bias for the binary mixture R1234yf (1) + R1233xf.

Reference	*T/K*	k_{12}	*AAD P /%*	*AAD* y_1 */%*	*bias P /%*	*bias* y_1 */%*
This work	298.31	0.0122	0.42	0.37	-0.29	-0.23
	323.27	0.0172	0.41	0.88	-0.41	-0.88
	348.25	0.01502	0.33	0.65	0.04	-0.65
Yang et al. 2016	293.15	0.0167	0.67	0.44	0.45	-0.41
	303.15	0.0174	0.66	0.14	0.57	-0.08
	313.15	0.0224	1.97	0.22	1.73	0.09

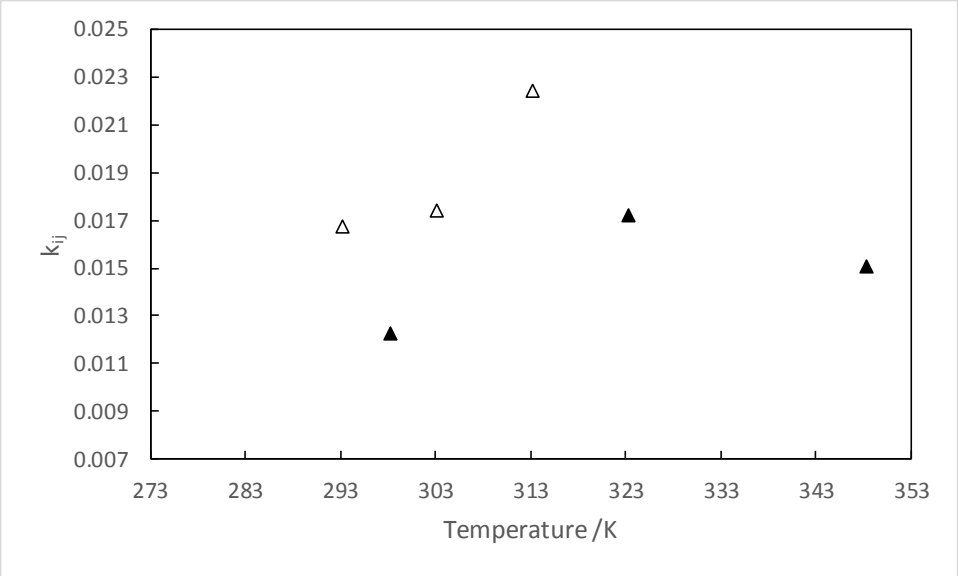

Figure 12: Variation of the binary interaction parameters (binary system R1234yf + R1233xf) with the temperature. (▲): this work, (Δ): Yang et al. (2016)

5. Conclusions

In this paper, the isothermal VLE of two systems, R1234yf + (R134a or R152a) were measured using a static-analytic apparatus at temperatures between 278.15 and 348.15 K. The experiments were conducted by means of a "static-analytic" apparatus with phase analysis via gas chromatography, with resulting uncertainties of 0.06 K for temperature, 8 kPa for pressure and a maximum of 0.007 for vapour and liquid mole fractions. All the uncertainties were estimated taking into account the purities of the chemicals. The data obtained were correlated within 5% of absolute error with a Peng-Robinson cubic equation of state associated with a Mathias-Copeman alpha function and the classical van der Waals mixing rules (with a temperature-dependent binary interaction parameter).

6. Acknowledgments

The authors are grateful to the French National Agency of Research (ANR) for funding this work as part of PREDIREF Project (ANR-13-CDII-0008).

7. References

Bell, I. H., Lemmon, E. W. 2016. Automatic fitting of binary interaction parameters for multi-fluid Helmholtz-energy-explicit mixture models. J. Chem. Eng. Data 61, 3752-3760. https://doi.org/10.1021/acs.jced.6b00257

Brown, J.S., Zilio, C., Cavallini, A., 2010. Critical review of the latest thermodynamic and transport property data and models, and equations of state for R-1234yf. International Refrigeration and Air Conditioning Conference, Purdue, Paper No. 1130

Coquelet, C., Richon, D. 2009. Experimental Determination of Phase Diagram and Modeling. Application to Refrigerant Mixtures. Int. J. Refrig. 32, 1604-1614. https://doi.org/10.1016/j.ijrefrig.2009.03.013

Coquelet, C., Valtz, A., Théveneau, P. 2019. Experimental Determination of Thermophysical Properties of Working Fluids for ORC Applications. ORC for Waste Heat Recovery Applications, IntechOpen, London, pp 17-43.

Directive 2006/40/EC of The European Parliament and of the Council of 17 May 2006 relating to emissions from air-conditioning systems in motor vehicles and amending Council Directive 70/156/EC. Official J. of the European Union, 2006. Retrieved online at: http://eur-lex.europa.eu/LexUriServ/LexUriServ.do?uri¼OJ:L:2006:161:0012:0018:EN:PDF,

November 8, 2011.

Dohrn, R., Peper, S., Fonseca, J. M. S. 2010. High-pressure fluid-phase equilibria: Experimental methods and systems investigated (2000–2004) Fluid Phase Equilib. 288, 1–54. https://doi.org/10.1016/j.fluid.2009.08.008

European Union Regulation (EC) No 842/2006 of The European Parliament and of the Council of 17 May 2006, Certain Fluorinated Greenhouse Gases, Official Journal of the European Union, 2006

Fonseca, J. M. S. , Dohrn, R., Peper, S. 2011. High-pressure fluid-phase equilibria: Experimental methods and systems investigated (2005–2008). Fluid Phase Equilib. 300, 1–69. https://doi.org/10.1016/j.fluid.2010.09.017

Hu, P., Chen, L.X., Zhu, W.B., Jia, L., Chen, Z.S. 2014. Isothermal VLE measurements for the binary mixture of 2,3,3,3-tetrafluoroprop-1-ene (HFO-1234yf)+1,1-difluoroethane (HFC-152a) Fluid Phase Equilib. 373,80–83. https://doi.org/10.1016/j.fluid.2014.04.015

Juntarachat, N., Valtz, A., Coquelet, C., Privat, R., Jaubert, J.-N. 2014. Experimental measurements and correlation of vapor–liquid equilibrium and critical data for the CO2 + R1234yf and CO2 + R1234ze(E) binary mixtures. Int. J. Refrig. 47, 141–152. https://doi.org/10.1016/j.ijrefrig.2014.09.001

Kamiaka, T., Dang, C., Hihara, E. 2013. Vapor-liquid equilibrium measurements for binary mixtures of R1234yf with R32, R125, and R134a Int. J. Refrig. 36, 965–971. https://doi.org/10.1016/j.ijrefrig.2012.08.016

Kwak, T. Y., Mansoori, G.A. 1986. Van der waals mixing rules for cubic equations of state. Applications for supercritical fluid extraction modelling. Chem. Eng. Sci. 41, 1303–1309. https://doi.org/10.1016/0009-2509(86)87103-2

Lasserre, V., Heyndrickx, F., Rivoallon, R., Guegan, L. 2014. Le réglement F-Gas, objectifs et impacts. Revue Générale du Froid, 1144, 22-27.

Lemmon, E.W., Bell, I.H., Huber, M.L., 2018. NIST Standard Reference Database 23: Reference Fluid Thermodynamic and Transport Properties REFPROP, version 10.0, National Institute of Standards and Technology (https://pages.nist.gov/REFPROP-docs/)

Liu, B., Rivière, P., Coquelet, C., Gicquel, R., David, F. 2012. Investigation of a two stage Rankine cycle for electric power plants Applied Energy 100, 285-294. https://doi.org/10.1016/j.apenergy.2012.05.044

Mathias, P. M. Copeman, T.W. 1983. Extension of the Peng-Robinson equation of state to complex mixtures: Evaluation of the various forms of the local composition concept. Fluid Phase Equilib. 13, 91–108. https://doi.org/10.1016/0378-3812(83)80084-3

McCulloch, A. 1999. CFC and Halon replacements in the environment J. Fluor. Chem. 100, 163–173. https://doi.org/10.1016/S0022-1139(99)00198-0

Minor, B., Spatz, M. 2008. International Refrigeration and Air Conditioning Conference, Purdue, Paper No. 2349

Peng, D.-Y., Robinson, D.B. 1976. A New Two-Constant Equation of State. Ind. Eng. Chem. Fundam. 15, 59–64. https:// 10.1016/0378-3812(85)87035-7

Scott, R.L., van Konynenburg, P.H. 1980. Critical lines and phase equilibria in binary van der Waals mixtures. Phil. Trans. R. Soc. London 298, 495–540. https://doi.org/10.1098/rsta.1980.0266

Taylor, B. N., Kuyatt, C.E. 2009. Guidelines for Evaluating and Expressing the Uncertainty of NIST Measurement Results (rev. Ed.), DIANE Publishing, Washington

Teinz, K., Manuel, S.R., Chen, B.B., Pigamo, A., Doucet, N., Kemnitz, E. 2015. Catalytic formation of 2, 3, 3, 3-tetrafluoropropene from 2-chloro-3, 3, 3-trifluoropropene at fluorinated chromia: A study of reaction pathways.Appl. Catal. B Environ. 165, 200-208. https://doi.org/10.1016/j.apcatb.2014.09.076

Valtz, A., El Abbadi, J., Coquelet, C., Houriez, C. 2019. Experimental measurements and modeling of vapour liquid equilibrium of 2,3,3,3 tetrafluoropropene (R1234yf) + 1,1,1,2,2 pentafluoropropane (R245cb) system. Int. J. Refrig. 107, 315-325. https://doi.org/10.1016/j.ijrefrig.2019.07.024

Wang, S., Fauve, R., Coquelet, C., Valtz, A., Houriez, C., Artola, P.A., El Ahmar, E., Rousseau, B., Hu, H. 2019. Vapor-liquid equilibrium and molecular simulation data for carbon dioxide (CO2) + trans-1,3,3,3-tetrafluoroprop-1-ene (R-1234ze(E)) mixture at temperatures from 283.32 to 353.02 K and pressures up to 7.6 MPa. Int J. of Refrig. 98, 362-371. https://doi.org/10.1016/j.ijrefrig.2018.10.032

Yamada, Y., Tsuchiya, T., Shibanuma, T. 2010. Environmentally friendly non-flammable refrigerants, International Symposium on Next-generation Air Conditioning and Refrigeration Technology Conference, Purdue.

Yang, T., Hu, X., Meng, X., Wu, J. 2018. Vapor–Liquid Equilibria for the Binary and Ternary Systems of Difluoromethane (R32), 1, 1-Difluoroethane (R152a), and 2, 3, 3, 3-Tetrafluoroprop-1-ene (R1234yf). J. Chem.Eng. Data 63, 771-780. https://doi.org/10.1021/acs.jced.7b00950

Yang, Z. Q., Kou, L. G., Lu, J., Zhang, W., Mao, W. Lu, J. 2016. Isothermal vapor–liquid equilibria measurements for binary systems of 2, 3, 3, 3-tetrafluoropropene (HFO-1234yf)+ 2-chloro-3, 3, 3-trifluoropropene (HCFO-1233xf) and 2-chloro-3, 3, 3-trifluoropropene (HCFO-1233xf)+ 2-chloro-1, 1, 1, 2-tetrafluoropropane (HCFC-244bb). Fluid Phase Equilib. 414, 143-148. ttps://doi.org/10.1016/j.fluid.2016.01.027

Zhang, W., Yang, Z. Q., Lu, J. Lu, J. 2013. Vapor pressures of 2-chloro-3, 3, 3-trifluoropropene (HCFO-1233xf). J. Chem. Eng. Data, 58, 2307-2310. https://doi.org/10.1021/je400407z